

Fenchel Duality Theory and a Primal-Dual Algorithm on Riemannian Manifolds

Ronny Bergmann^a, Roland Herzog^a,
José Vidal-Núñez^a, Daniel Tenbrinck^b

^aTechnische Universität Chemnitz, Chemnitz, Germany

^bFriedrich-Alexander-Universität, Erlangen, Germany.

Oberseminar Applied Algebra and Analysis
Institut für Analysis und Algebra, TU Braunschweig.

Braunschweig, December 10, 2019.

Contents

1. Introduction
2. Fenchel Duality
3. The Chambolle–Pock Algorithm
4. Numerical Examples
5. Summary & Conclusion

1. Introduction

Manifold-Valued Signals and Images

New data acquisition modalities lead to non-Euclidean range

- Interferometric synthetic aperture radar (InSAR)
- Surface normals, GPS data, wind, flow,...
- Diffusion tensors in magnetic resonance imaging (DT-MRI), covariance matrices
- Electron backscattered diffraction (EBSD)



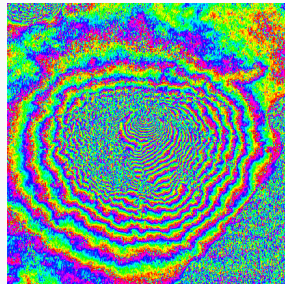
InSAR-Data of Mt. Vesuvius
[Rocca, Prati, Guarneri, 1997]

phase-valued data, $\mathcal{M} = \mathbb{S}^1$

Manifold-Valued Signals and Images

New data acquisition modalities lead to non-Euclidean range

- Interferometric synthetic aperture radar (InSAR)
- Surface normals, GPS data, wind, flow,...
- Diffusion tensors in magnetic resonance imaging (DT-MRI), covariance matrices
- Electron backscattered diffraction (EBSD)



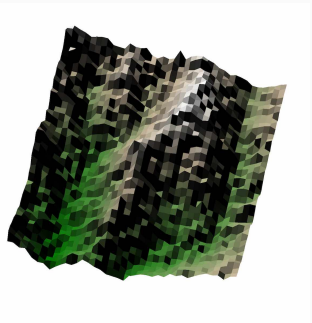
InSAR-Data of Mt. Vesuvius
[Rocca, Prati, Guarneri, 1997]

phase-valued data, $\mathcal{M} = \mathbb{S}^1$

Manifold-Valued Signals and Images

New data acquisition modalities lead to non-Euclidean range

- Interferometric synthetic aperture radar (InSAR)
- Surface normals, GPS data, wind, flow,...
- Diffusion tensors in magnetic resonance imaging (DT-MRI), covariance matrices
- Electron backscattered diffraction (EBSD)

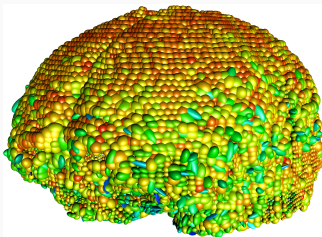


National elevation dataset
[Gesch et al., 2009]
directional data, $\mathcal{M} = \mathbb{S}^2$

Manifold-Valued Signals and Images

New data acquisition modalities lead to non-Euclidean range

- Interferometric synthetic aperture radar (InSAR)
- Surface normals, GPS data, wind, flow,...
- Diffusion tensors in magnetic resonance imaging (DT-MRI), covariance matrices
- Electron backscattered diffraction (EBSD)

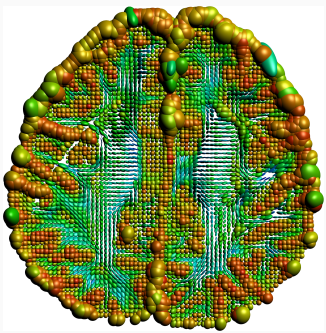


diffusion tensors in human brain
from the Camino dataset
<http://cmic.cs.ucl.ac.uk/camino>
sym. pos. def. matrices, $\mathcal{M} = \text{SPD}(3)$

Manifold-Valued Signals and Images

New data acquisition modalities lead to non-Euclidean range

- Interferometric synthetic aperture radar (InSAR)
- Surface normals, GPS data, wind, flow,...
- Diffusion tensors in magnetic resonance imaging (DT-MRI), covariance matrices
- Electron backscattered diffraction (EBSD)



horizontal slice #28
from the Camino dataset
<http://cmic.cs.ucl.ac.uk/camino>
sym. pos. def. matrices, $\mathcal{M} = \text{SPD}(3)$

Manifold-Valued Signals and Images

New data acquisition modalities lead to non-Euclidean range

- Interferometric synthetic aperture radar (InSAR)
- Surface normals, GPS data, wind, flow,...
- Diffusion tensors in magnetic resonance imaging (DT-MRI), covariance matrices
- Electron backscattered diffraction (EBSD)



EBSD example from the MTEX toolbox
[Bachmann, Hielscher, since 2005]

Rotations (mod. symmetry),
 $\mathcal{M} = \text{SO}(3)(/\mathcal{S})$.

Manifold-Valued Signals and Images

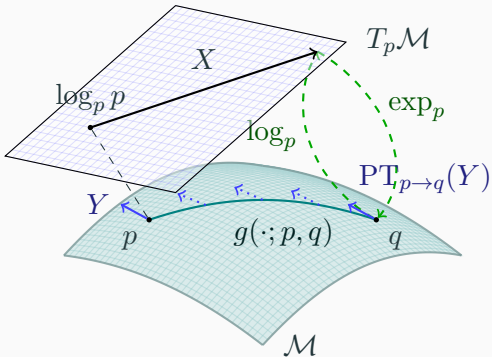
New data acquisition modalities lead to non-Euclidean range

- Interferometric synthetic aperture radar (InSAR)
- Surface normals, GPS data, wind, flow,...
- Diffusion tensors in magnetic resonance imaging (DT-MRI), covariance matrices
- Electron backscattered diffraction (EBSD)

Common properties

- Range of values is a Riemannian manifold
- Tasks from “classical” image processing, e.g.
 - denoising
 - inpainting
 - interpolation
 - labeling
 - deblurring

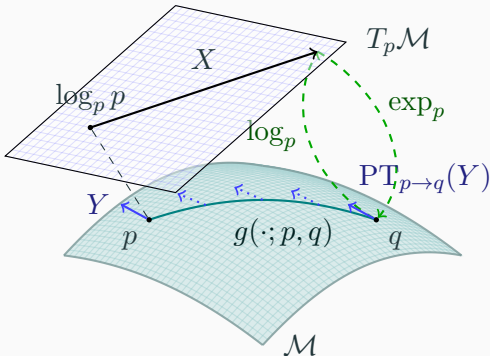
A d -dimensional Riemannian Manifold \mathcal{M}



A d -dimensional Riemannian manifold can be informally defined as a set \mathcal{M} covered with a ‘suitable’ collection of charts, that identify subsets of \mathcal{M} with open subsets of \mathbb{R}^d and a continuously varying inner product on the tangential spaces.

[Absil, Mahony, Sepulchre, 2008]

A d -dimensional Riemannian Manifold \mathcal{M}



Geodesic $g(\cdot; p, q)$ shortest path (on \mathcal{M}) between $p, q \in \mathcal{M}$

Tangent space $T_p\mathcal{M}$ at p , with inner product $(\cdot, \cdot)_p$

Logarithmic map $\log_p q = \dot{g}(0; p, q)$ “speed towards q ”

Exponential map $\exp_p X = g(1)$, where $g(0) = p$, $\dot{g}(0) = X$

Parallel transport $\text{PT}_{p \rightarrow q}(Y)$ of $Y \in T_p\mathcal{M}$ along $g(\cdot; p, q)$

The Model

We consider the minimization problem

$$\arg \min_{p \in \mathcal{C}} F(p) + G(\Lambda(p))$$

- \mathcal{M}, \mathcal{N} are (high-dimensional) Riemannian Manifolds
- $F: \mathcal{M} \rightarrow \overline{\mathbb{R}}$ (locally) convex, nonsmooth
- $G: \mathcal{N} \rightarrow \overline{\mathbb{R}}$ (locally) convex, nonsmooth
- $\Lambda: \mathcal{M} \rightarrow \mathcal{N}$ nonlinear
- $\mathcal{C} \subset \mathcal{M}$ strongly geodesically convex.

Splitting Methods & Algorithms

On a Riemannian manifold \mathcal{M} we have

- Cyclic Proximal Point Algorithm (CPPA)
- (parallel) Douglas–Rachford Algorithm (PDRA)

[Bačák, 2014]

[Bergmann, Persch, Steidl, 2016]

On \mathbb{R}^n PDRA is known to be equivalent to

[Setzer, 2011; O'Connor, Vandenberghe, 2018]

- Primal-Dual Hybrid Gradient Algorithm (PDHGA)

[Esser, Zhang, Chan, 2010]

- Chambolle-Pock Algorithm (CPA)

[Chambolle, Pock, 2011; Pock et al., 2009]

Goals of this talk.

Formulate Duality on a Manifold

Derive a Riemannian Chambolle–Pock Algorithm (RCPA)

Musical Isomorphisms

[Lee, 2003]

The dual space $\mathcal{T}_p^*\mathcal{M}$ of a tangent space $\mathcal{T}_p\mathcal{M}$ is called **cotangent space**. We denote by $\langle \cdot, \cdot \rangle$ the duality pairing.

We define the **musical isomorphisms**

- $\flat: \mathcal{T}_p\mathcal{M} \ni X \mapsto X^\flat \in \mathcal{T}_p^*\mathcal{M}$ via $\langle X^\flat, Y \rangle = (X, Y)_p$
for all $Y \in \mathcal{T}_p\mathcal{M}$
- $\sharp: \mathcal{T}_p^*\mathcal{M} \ni \xi \mapsto \xi^\sharp \in \mathcal{T}_p\mathcal{M}$ via $(\xi^\sharp, Y)_p = \langle \xi, Y \rangle$
for all $Y \in \mathcal{T}_p\mathcal{M}$.

\Rightarrow inner product and parallel transport on/between $\mathcal{T}_p^*\mathcal{M}$

Convexity

[Sakai, 1996; Udrişte, 1994]

A set $\mathcal{C} \subset \mathcal{M}$ is called (strongly geodesically) **convex** if for all $p, q \in \mathcal{C}$ the geodesic $g(\cdot; p, q)$ is unique and lies in \mathcal{C} .

A function $F: \mathcal{C} \rightarrow \overline{\mathbb{R}}$ is called **convex** if for all $p, q \in \mathcal{C}$ the composition $F(g(t; p, q)), t \in [0, 1]$, is convex.

The Subdifferential

[Lee, 2003; Udrişte, 1994]

The **subdifferential** of F at $p \in \mathcal{C}$ is given by

$$\partial_{\mathcal{M}} F(p) := \{\xi \in \mathcal{T}_p^* \mathcal{M} \mid F(q) \geq F(p) + \langle \xi, \log_p q \rangle \text{ for } q \in \mathcal{C}\},$$

where

- $\mathcal{T}_p^* \mathcal{M}$ is the dual space of $\mathcal{T}_p \mathcal{M}$,
- $\langle \cdot, \cdot \rangle$ denotes the duality pairing on $\mathcal{T}_p^* \mathcal{M} \times \mathcal{T}_p \mathcal{M}$

2. Fenchel Duality

The Euclidean Fenchel Conjugate

Let $f: \mathbb{R}^n \rightarrow \overline{\mathbb{R}}$ be proper and convex.

We define the **Fenchel conjugate** $f^*: \mathbb{R}^n \rightarrow \overline{\mathbb{R}}$ of f by

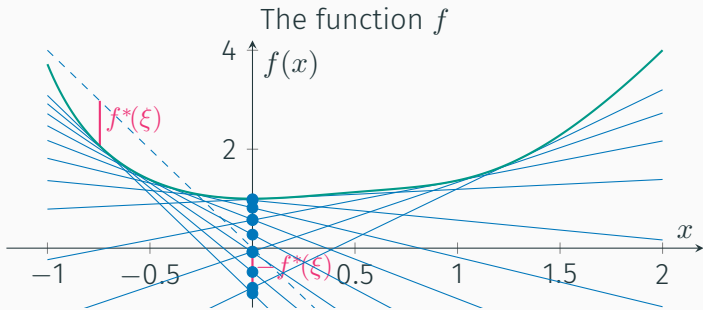
$$f^*(\xi) := \sup_{x \in \mathbb{R}^n} \langle \xi, x \rangle - f(x) = \sup_{x \in \mathbb{R}^n} \begin{pmatrix} \xi \\ -1 \end{pmatrix}^T \begin{pmatrix} x \\ f(x) \end{pmatrix}$$

- interpretation: maximize the distance of $\xi^T x$ to f
 \Rightarrow extremum seeking problem on the epigraph

The Fenchel biconjugate reads

$$f^{**}(x) = (f^*)^*(x) = \sup_{\xi \in \mathbb{R}^n} \{ \langle \xi, x \rangle - f^*(\xi) \}.$$

Illustration of the Fenchel Conjugate



The Fenchel conjugate f^*



Properties of the Fenchel Conjugate

[Rockafellar, 1970]

- The Fenchel conjugate f^* is **convex** (even if f is not)
- If $f(x) \leq g(x)$ holds for all $x \in \mathbb{R}^n$
then $f^*(\xi) \geq g^*(\xi)$ holds for all $\xi \in \mathbb{R}^n$
- If $g(x) = f(x + b)$ for some $b \in \mathbb{R}$ holds for all $x \in \mathbb{R}^n$
then $g^*(\xi) = f^*(\xi) - \xi^T b$ holds for all $\xi \in \mathbb{R}^n$
- If $g(x) = \lambda f(x)$, for some $\lambda > 0$, holds for all $x \in \mathbb{R}^n$
then $g^*(\xi) = \lambda f^*(\xi/\lambda)$ holds for all $\xi \in \mathbb{R}^n$
- f^{**} is the largest convex, lsc function with $f^{**} \leq f$
- especially the **Fenchel–Moreau theorem**:
 f convex, proper, lsc $\Rightarrow f^{**} = f$.

Properties of the Fenchel Conjugate II

The Fenchel–Young inequality holds, i.e.,

$$f(x) + f^*(\xi) \geq \xi^T x \quad \text{for all } x, \xi \in \mathbb{R}^n$$

We can characterize subdifferentials

- For a proper, convex function f

$$\xi \in \partial f(x) \Leftrightarrow f(x) + f^*(\xi) = \xi^T x$$

- For a proper, convex, lsc function f , then

$$\xi \in \partial f(x) \Leftrightarrow x \in \partial f^*(\xi)$$

The Riemannian m -Fenchel Conjugate

[Bergmann et al., 2019]

alternative approach: [Ahmadi Kakavandi, Amini, 2010]

Idea: Introduce a point on \mathcal{M} to “act as” 0.

Let $m \in \mathcal{C} \subset \mathcal{M}$ be given and $F: \mathcal{C} \rightarrow \overline{\mathbb{R}}$.

The **m -Fenchel conjugate** $F_m^*: \mathcal{T}_m^*\mathcal{M} \rightarrow \overline{\mathbb{R}}$ is defined by

$$F_m^*(\xi_m) := \sup_{X \in \mathcal{L}_{\mathcal{C},m}} \{ \langle \xi_m, X \rangle - F(\exp_m X) \},$$

where

$$\mathcal{L}_{\mathcal{C},m} := \{X \in \mathcal{T}_m\mathcal{M} \mid q = \exp_m X \in \mathcal{C} \text{ and } \|X\|_p = d(q, p)\}.$$

Let $m' \in \mathcal{C}$.

The **mm' -Fenchel-biconjugate** $F_{mm'}^{**}: \mathcal{C} \rightarrow \overline{\mathbb{R}}$ is given by,

$$F_{mm'}^{**}(p) = \sup_{\xi_{m'} \in \mathcal{T}_{m'}^*\mathcal{M}} \{ \langle \xi_{m'}, \log_{m'} p \rangle - F_m^*(\mathcal{P}_{m' \rightarrow m} \xi_{m'}) \}.$$

Properties of the m -Fenchel Conjugate

- F_m^* is convex on $\mathcal{T}_m^*\mathcal{M}$
- If $F(p) \leq G(p)$ holds for all $p \in \mathcal{C}$
then $F_m^*(\xi) \geq G_m^*(\xi_m)$ holds for all $\xi_m \in \mathcal{T}_m^*\mathcal{M}$
- If $G(x) = F(x) + a$ for some $a \in \mathbb{R}$ holds for all $p \in \mathcal{C}$
then $G_m^*(\xi_m) = F_m^*(\xi_m) - a$ holds for all $\xi_m \in \mathcal{T}_m^*\mathcal{M}$
- If $G(p) = \lambda F(p)$, for some $\lambda > 0$, holds for all $p \in \mathcal{C}$
then $G_m^*(\xi_m) = \lambda F_m^*(\xi_m/\lambda)$ holds for all $\xi_m \in \mathcal{T}_m^*\mathcal{M}$
- It holds $F_{mm}^{**} \leq F$ on \mathcal{C}
- especially the **Fenchel-Moreau theorem**:
If F convex, proper, lsc then $F_{mm}^{**} = F$ on \mathcal{C} .

Properties of the m -Fenchel Conjugate II

The Fenchel–Young inequality holds, i.e.,

$$F(p) + F_m^*(\xi_m) \geq \langle \xi_m, \log_m p \rangle \quad \text{for all } p \in \mathcal{C}, \xi_m \in \mathcal{T}_m^* \mathcal{M}$$

We can characterize subdifferentials

- For a proper, convex function F

$$\xi_p \in \partial_{\mathcal{M}} F(p) \Leftrightarrow F(p) + F_m^*(\mathcal{P}_{p \rightarrow m} \xi_p) = \langle \mathcal{P}_{p \rightarrow m} \xi_p, \log_m p \rangle.$$

- For a proper, convex, lsc function F

$$\xi_p \in \partial_{\mathcal{M}} F(p) \Leftrightarrow \log_m p \in \partial F_m^*(\mathcal{P}_{p \rightarrow m} \xi_p).$$

3. The Chambolle–Pock Algorithm

The Euclidean Chambolle–Pock Algorithm

[Chambolle, Pock, 2011]

From the pair of primal-dual problems

$$\min_{x \in \mathbb{R}^n} f(x) + g(Kx), \quad K \text{ linear},$$

$$\max_{\xi \in \mathbb{R}^m} -f^*(-K^*\xi) - g^*(\xi)$$

we obtain for f, g proper convex, lsc the optimality conditions (OC) for a solution $(\hat{x}, \hat{\xi})$ as

$$\partial f \ni -K^*\hat{\xi}$$

$$\partial g^*(\hat{\xi}) \ni K\hat{x}$$

The Euclidean Chambolle–Pock Algorithm

[Chambolle, Pock, 2011]

From the pair of primal-dual problems

$$\min_{x \in \mathbb{R}^n} f(x) + g(Kx), \quad K \text{ linear},$$

$$\max_{\xi \in \mathbb{R}^m} -f^*(-K^*\xi) - g^*(\xi)$$

we obtain for f, g proper convex, lsc the

Chambolle–Pock Algorithm. with $\sigma > 0, \tau > 0, \theta \in \mathbb{R}$

$$\begin{aligned} x^{(k+1)} &= \text{prox}_{\sigma f}(x^{(k)} - \sigma K^* \bar{\xi}^{(k)}) \\ \xi^{(k+1)} &= \text{prox}_{\tau g^*}(\xi^{(k)} + \tau K x^{(k+1)}) \\ \bar{\xi}^{(k+1)} &= \xi^{(k+1)} + \theta(\xi^{(k+1)} - \xi^{(k)}) \end{aligned}$$

Proximal Map

For $F: \mathcal{M} \rightarrow \overline{\mathbb{R}}$ and $\lambda > 0$ we define the **Proximal Map** as

[Moreau, 1965; Rockafellar, 1976; Ferreira, Oliveira, 2002]

$$\text{prox}_{\lambda F}(p) := \arg \min_{u \in \mathcal{M}} d(u, p)^2 + \lambda F(u).$$

! For a Minimizer u^* of F we have $\text{prox}_{\lambda F}(u^*) = u^*$.

- For F proper, convex, lsc:
 - the proximal map is unique.
 - PPA $x_k = \text{prox}_{\lambda F}(x_{k-1})$ converges to $\arg \min F$
- $q = \text{prox}_{\lambda F}(p)$ is equivalent to

$$\frac{1}{\lambda} (\log_q p)^\flat \in \partial_{\mathcal{M}} F(q)$$

Saddle Point Formulation

From

$$\min_{p \in \mathcal{C}} F(p) + G(\Lambda(p))$$

we derive the saddle point formulation for the n -Fenchel conjugate of G as

$$\min_{p \in \mathcal{C}} \max_{\xi_n \in \mathcal{T}_n^* \mathcal{N}} \langle \xi_n, \log_n \Lambda(p) \rangle + F(p) - G_n^*(\xi_n).$$

For Optimality Conditions and the Dual Problem: What's Λ^* ?

Approach. Linearization:

on \mathbb{R}^n : [Valkonen, 2014]

$$\Lambda(p) \approx \exp_{\Lambda(m)} D\Lambda(m)[\log_m p]$$

Optimality Conditions for the Saddle Point Problem

The first order optimality conditions for a saddle point of the **exact** saddle point problem

$$(\hat{p}, \hat{\xi}_n) \in \mathcal{C} \times \mathcal{T}_n^* \mathcal{N}$$

can be formally derived as

$$\begin{aligned}\mathcal{P}_{m \rightarrow \hat{p}} - (D\Lambda)^*[\hat{\xi}_n] &\in \partial_{\mathcal{M}} F(\hat{p}) \\ \log_n \Lambda(\hat{p}) &\in \partial G_n^*(\hat{\xi}_n)\end{aligned}$$

Advantage. By only linearizing for the adjoint, we stay closer to the original problem.

Linearization & the Dual Problem

Linearizing the primal problem obtain e.g. for $n = \Lambda(m)$

Primal Problem.

$$\min_{p \in \mathcal{C}} F(p) + G(\exp_{\Lambda(m)} D\Lambda(m)[\log_m p])$$

Saddle Point Problem.

$$\min_{p \in \mathcal{C}} \max_{\xi_n \in \mathcal{T}_n^* \mathcal{N}} \langle D\Lambda(m)^*[\xi_n], \log_m p \rangle + F(p) - G_n^*(\xi_n).$$

Dual Problem.

$$\max_{\xi_n \in \mathcal{T}_n^* \mathcal{N}} -F_m^*(-D\Lambda(m)^*[\xi_n]) - G_n^*(\xi_n).$$

and a classical duality theory including weak duality.

Optimality Conditions for the Saddle Point Problem

The first order optimality conditions for a saddle point of the linearized problem

$$(\hat{p}, \hat{\xi}_n) \in \mathcal{C} \times \mathcal{T}_n^* \mathcal{N}$$

can be formally derived as

$$\mathcal{P}_{m \rightarrow \hat{p}} - (D\Lambda)^*[\hat{\xi}_n] \in \partial_{\mathcal{M}} F(\hat{p})$$

$$D\Lambda(m)[\log_m \hat{p}] \in \partial G_n^*(\hat{\xi}_n)$$

Advantage. A complete duality theory and a certain symmetry in the optimality conditions.

For $\mathcal{M} = \mathbb{R}^d$ and $K = \Lambda$ linear both approaches yield the classical conditions

$$-K^* \hat{\xi} \in \partial F(\hat{p})$$

$$K \hat{p} \in \partial G^*(\hat{\xi})$$

The exact Riemannian Chambolle–Pock Algorithm (eRCPA)

Input: $m, p^{(0)} \in \mathcal{C} \subset \mathcal{M}$, $n = \Lambda(m)$, $\xi_n^{(0)} \in \mathcal{T}_n^* \mathcal{N}$,
and parameters $\sigma, \tau, \theta > 0$

1: $k \leftarrow 0$

2: $\bar{p}^{(0)} \leftarrow p^{(0)}$

3: **while** not converged **do**

4: $\xi_n^{(k+1)} \leftarrow \text{prox}_{\tau G_n^*} \left(\xi_n^{(k)} + \tau \left(\log_n \Lambda(\bar{p}^{(k)}) \right)^\flat \right)$

5: $p^{(k+1)} \leftarrow \text{prox}_{\sigma F} \left(\exp_{p^{(k)}} \left(\mathcal{P}_{m \rightarrow p^{(k)}} \left(-\sigma D\Lambda(m)^* [\xi_n^{(k+1)}]^\sharp \right) \right) \right)$

6: $\bar{p}^{(k+1)} \leftarrow \exp_{p^{(k+1)}} \left(-\theta \log_{p^{(k+1)}} p^{(k)} \right)$

7: $k \leftarrow k + 1$

8: **end while**

Output: $p^{(k)}$

Generalizations & Variants of the RCPA

Classically

[Chambolle, Pock, 2011]

- change $\sigma = \sigma_k, \tau = \tau_k, \theta = \theta_k$ during the iterations
- introduce an acceleration γ
- relax **dual** $\bar{\xi}$ instead of **primal** \bar{p} (switches lines 4 and 5)

Furthermore we

[Bergmann et al., 2019]

- introduce the **lRCPA**: linearize Λ , too, i.e.

$$\log_n \Lambda(\bar{p}^{(k)}) \quad \rightarrow \quad \mathcal{P}_{\Lambda(m) \rightarrow n} D\Lambda(m)[\log_m \bar{p}^{(k)}]$$

- choose $n \neq \Lambda(m)$ introduces a parallel transport

$$D\Lambda(m)^*[\xi_n^{(k+1)}] \quad \rightarrow \quad D\Lambda(m)^*[\mathcal{P}_{n \rightarrow \Lambda(m)} \xi_n^{(k+1)}]$$

- change $m = m^{(k)}, n = n^{(k)}$ during the iterations

The Linearized Riemannian Chambolle–Pock Algorithm (lRCPA)

Input: $m, p^{(0)} \in \mathcal{C} \subset \mathcal{M}$, $n = \Lambda(m)$, $\xi_n^{(0)} \in \mathcal{T}_n^* \mathcal{N}$,
and parameters $\sigma, \tau, \theta > 0$

1: $k \leftarrow 0$

2: $\bar{\xi}_n^{(0)} \leftarrow \xi_n^{(0)}$

3: **while** not converged **do**

4: $p^{(k+1)} \leftarrow \text{prox}_{\sigma F} \left(\exp_{p^{(k)}} \left(\mathcal{P}_{m \rightarrow p^{(k)}} \left(-\sigma D\Lambda(m)^* [\bar{\xi}_n^{(k)}] \right)^\sharp \right) \right)$

5: $\xi_n^{(k+1)} \leftarrow \text{prox}_{\tau G_n^*} \left(\xi_n^{(k)} + \tau (D\Lambda(p^{(k+1)}))^\flat \right)$

6: $\bar{\xi}_n^{(k)} \leftarrow \xi_n^{(k)} + \theta (\xi_n^{(k)} - \xi_n^{(k-1)}).$

7: $k \leftarrow k + 1$

8: **end while**

Output: $p^{(k)}$

The Linearized RCPA with Dual Relaxation

We introduce for ease of notation

$$\tilde{p}^{(k)} = \exp_{p^{(k)}} \left(\mathcal{P}_{m \rightarrow p^{(k)}} - (\sigma(D\Lambda(m))^*[\bar{\xi}_n^{(k)}])^\sharp \right)$$

for the **linearized** Riemannian Chambolle Pock
with **dual relaxed**

$$\bar{\xi}_n^{(k)} \leftarrow \xi_n^{(k)} + \theta(\xi_n^{(k)} - \xi_n^{(k-1)}).$$

Especially for $\theta = 1$ we obtain

$$\bar{\xi}_n^{(k)} = 2\xi_n^{(k)} - \xi_n^{(k-1)}.$$

A Conjecture

We define

$$C(k) := \frac{1}{\sigma} d^2(p^{(k)}, \tilde{p}^{(k)}) + \langle \bar{\xi}_n^{(k)}, D\Lambda(m)[\zeta_k] \rangle,$$

where

$$\zeta_k = \mathcal{P}_{p^{(k)} \rightarrow m} (\log_{p^{(k)}} p^{(k+1)} - \mathcal{P}_{\tilde{p}^{(k)} \rightarrow p^{(k)}} \log_{\tilde{p}^{(k)}} \hat{p}) - \log_m p^{(k+1)} + \log_m \hat{p},$$

and \hat{p} is a minimizer of the primal problem.

Remark.

$$\text{For } \mathcal{M} = \mathbb{R}^d: \zeta_k = \tilde{p}^{(k)} - p^{(k)} = -\sigma(D\Lambda(m))^*[\bar{\xi}_n^{(k)}] \Rightarrow C(k) = 0.$$

Conjecture.

Assume $\sigma\tau < \|D\Lambda(m)\|^2$. Then $C(k) \geq 0$ for all $k > K$, $K \in \mathbb{N}$.

Convergence of the lRCPA

Theorem.

[Bergmann et al, 2019]

Let \mathcal{M}, \mathcal{N} be Hadamard. Assume that the linearized problem

$$\min_{p \in \mathcal{M}} \max_{\xi_n \in \mathcal{T}_n^* \mathcal{N}} \langle (D\Lambda(m))^* [\mathcal{P}_{n \rightarrow \Lambda(m)} \xi_n], \log_m p \rangle + F(p) - G_n^*(\xi_n).$$

has a saddle point $(\hat{p}, \hat{\xi}_n)$. Choose σ, τ such that

$$\sigma\tau < \|D\Lambda(m)\|^2$$

and assume that $C(k) \geq 0$ for all $k > K$. Then it holds

1. the sequence $(p^{(k)}, \xi_n^{(k)})$ remains bounded,
2. there exists a saddle-point (p', ξ'_n)
such that $p^{(k)} \rightarrow p'$ and $\xi_n^{(k)} \rightarrow \xi'_n$.

4. Numerical Examples

The ℓ^2 -TV Model

[Rudin, Osher, Fatemi, 1992; Lellmann et al., 2013; Weinmann, Demaret, Storath, 2014]

For a manifold-valued image $f \in \mathcal{M}$, $\mathcal{M} = \mathcal{N}^{d_1, d_2}$, we compute

$$\arg \min_{p \in \mathcal{M}} \frac{1}{\alpha} F(p) + G(\Lambda(p)), \quad \alpha > 0,$$

with

- data term $F(p) = \frac{1}{2} d_{\mathcal{M}}^2(p, f)$
 - “forward differences” $\Lambda: \mathcal{M} \rightarrow (\mathcal{T}\mathcal{N})^{d_1-1, d_2-1, 2}$,
- $$p \mapsto \Lambda(p) = \left((\log_{p_i} p_{i+e_1}, \log_{p_i} p_{i+e_2}) \right)_{i \in \{1, \dots, d_1-1\} \times \{1, \dots, d_2-1\}}$$
- prior $G(X) = \|X\|_{g,q,1}$ similar to a collaborative TV

[Duran et al., 2016]

The $d \times d$ Symmetric Positive Definite Matrices $\mathcal{P}(d)$.

$$\mathcal{P}(d) = \{p \in \mathbb{R}^{d \times d} \mid x^T p x > 0 \quad \text{for all } 0 \neq x \in \mathbb{R}^d\}$$

Tangent Space. $\mathcal{T}_p \mathcal{P}(d) = \left\{ p^{\frac{1}{2}} X p^{\frac{1}{2}} \mid X \in \mathbb{R}^{d \times d} \text{ with } X = X^T \right\}$

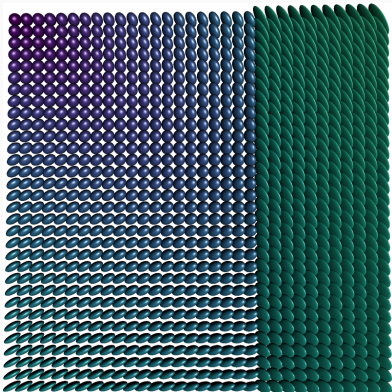
Riemannian Metric. $(X, Y)_p = \text{tr}(p^{-1} X p^{-1} Y),$

Exponential Map. $\exp_p X = p^{\frac{1}{2}} \text{Exp}(p^{-\frac{1}{2}} X p^{-\frac{1}{2}}) p^{\frac{1}{2}},$
where Exp is the matrix exponential.

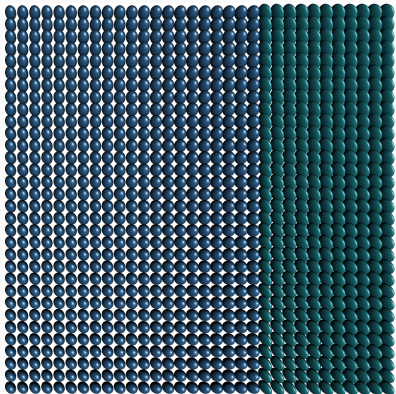
Parallel Transport. $P_{p \rightarrow q}(X) = p^{\frac{1}{2}} X' p^{-\frac{1}{2}} X p^{-\frac{1}{2}} X' p^{\frac{1}{2}},$
 $X' = \text{Exp}\left(\frac{1}{2} p^{-\frac{1}{2}} \log_p(q) p^{-\frac{1}{2}}\right),$
where \log is the logarithmic map.

The main tool to compute the matrix square root is the SVD.

Numerical Example for a $\mathcal{P}(3)$ -valued Image



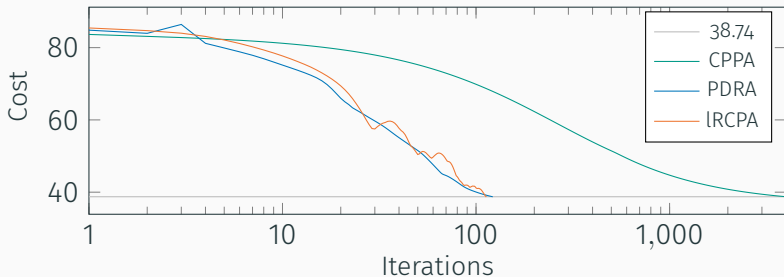
$\mathcal{P}(3)$ -valued data.



anisotropic TV, $\alpha = 6$.

- in each **pixel** we have a symmetric positive definite matrix
- Applications: denoising/inpainting e.g. of DT-MRI data

Numerical Example for a $\mathcal{P}(3)$ -valued Image

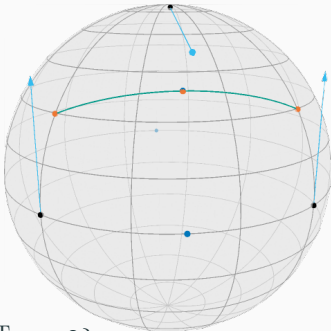


Approach. CPPA as benchmark

| | CPPA | PDRA | IRCPA |
|-------------------|---|--|-----------------------|
| parameters | $\lambda_k = \frac{4}{k}$ $\lambda = 0.93$ | $\eta = 0.58$ $\gamma = 0.2, m = I$ | $\sigma = \tau = 0.4$ |
| iterations | 4000 | 122 | 113 |
| runtime | 1235 s. | 380 s. | 96.1 s. |

The Sphere \mathbb{S}^d as a Manifold

$$\mathbb{S}^d = \{p \in \mathbb{R}^{d+1} \mid \|p\| = 1\}$$



Tangent Space. $\mathcal{T}_p \mathbb{S}^d = \{X \in \mathbb{R}^{d+1} \mid X^T p = 0\}$

Riemannian Metric. $(X, Y)_p = \langle X, Y \rangle$ from the embedding

Distance. $d_{\mathbb{S}^d}(p, q) = \arccos(\langle p, q \rangle)$

Exponential Map. $\exp_p X = \cos(\|X\|_2)p + \sin(\|X\|_2) \frac{X}{\|X\|_2}$

Parallel Transport. $P_{p \rightarrow q}(X) = X - \frac{\langle \log_p q, X \rangle_x}{d_{\mathbb{S}^d}^2(p, q)} (\log_p q + \log_q p).$

Base point Effect on \mathbb{S}^2 -valued data

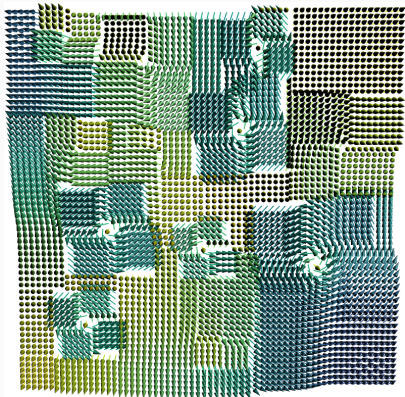


Original data

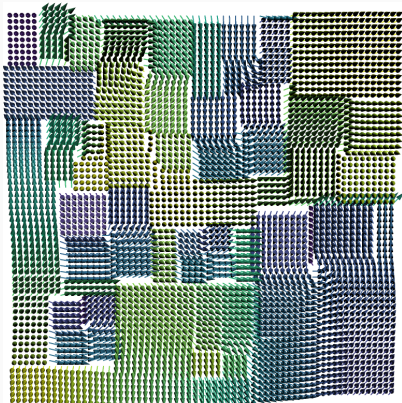


Original data

Base point Effect on \mathbb{S}^2 -valued data



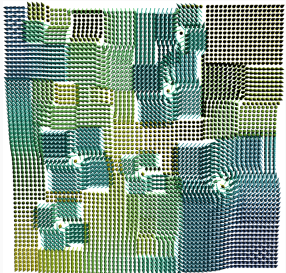
Result, m the mean (p. Px.)



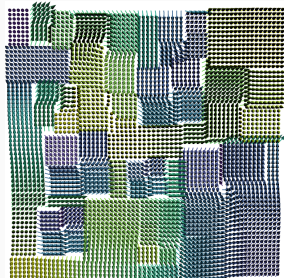
Result, m west (p. Px.)

- piecewise constant results for both
- ! different linearizations lead to different models

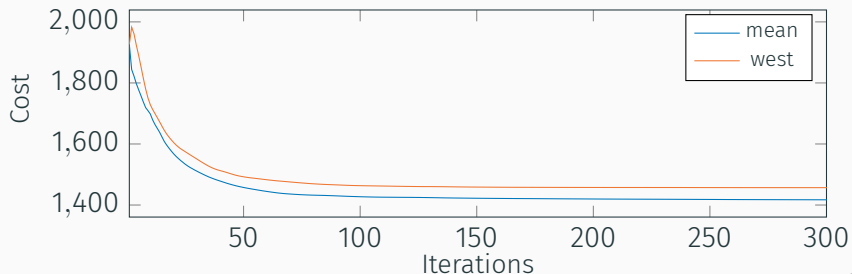
Base point Effect on \mathbb{S}^2 -valued data



Result, m the mean (p. Px.)



Result, m west (p. Px.)



5. Summary & Conclusion

Summary & Outlook

Summary.

- We introduced a duality framework on Riemannian manifolds
- We derived a Riemannian Chambolle Pock Algorithm
- Numerical example illustrates performance

Outlook.

- investigate $C(k)$
- strategies for choosing m, n (adaptively)
- investigate linearization error
- extend algorithm to graph-structured data

Reproducible Research

The algorithm will be published in `Manopt.jl`, a **Julia** Package available at <http://manoptjl.org>.

Goal.

Being able to use an(y) algorithm for a(ny) model directly on a(ny) manifold easily and efficiently.

Alternatives.

Manopt – manopt.org
(Matlab, N. Boumal)

pymanopt – [pymanopt.github.io](https://github.com/pymanopt/pymanopt)
(Python, S. Weichwald et. al.)

Example.

```
p0pt = linearizedChambollePock(M, N, cost,  
p, ξ, m, n, DΛ, AdjDΛ, proxF, proxConjG, σ, τ)
```

Reproducible Research

The algorithm will be published in `Manopt.jl`, a **Julia** Package available at <http://manoptjl.org>.

Goal.

Being able to use an(y) algorithm for a(ny) model directly on a(ny) manifold easily and efficiently.

Alternatives.

Manopt – manopt.org
(Matlab, N. Boumal)

pymanopt – pymanopt.github.io
(Python, S. Weichwald et. al.)

Example.

```
p0pt = exactChambollePock(M, N, cost,  
p, ξ, m, n, Λ, AdjΛ, proxF, proxConjG, σ, τ)
```

Selected References

-  Absil, P.-A.; Mahony, R.; Sepulchre, R. (2008). *Optimization Algorithms on Matrix Manifolds*. Princeton University Press. doi: 10.1515/9781400830244.
-  Bačák, M. (2014). "Computing medians and means in Hadamard spaces". *SIAM Journal on Optimization* 24.3, pp. 1542–1566. doi: 10.1137/140953393.
-  Bergmann, R.; Persch, J.; Steidl, G. (2016). "A parallel Douglas Rachford algorithm for minimizing ROF-like functionals on images with values in symmetric Hadamard manifolds". *SIAM Journal on Imaging Sciences* 9.4, pp. 901–937. doi: 10.1137/15M1052858.
-  Bergmann, R.; Herzog, R.; Tenbrinck, D.; Vidal-Núñez, J. (2019). *Fenchel Duality Theory and A Primal-Dual Algorithm on Riemannian Manifolds*. arXiv: 1908.02022.
-  Chambolle, A.; Pock, T. (2011). "A first-order primal-dual algorithm for convex problems with applications to imaging". *Journal of Mathematical Imaging and Vision* 40.1, pp. 120–145. doi: 10.1007/s10851-010-0251-1.
-  Rockafellar, R. T. (1970). *Convex analysis*. Princeton Mathematical Series, No. 28. Princeton University Press, Princeton, N.J.

 ronnybergmann.net/talks/2019-Braunschweig-RiemannianChambollePock.pdf